Simple colorimetric screening of paraquat residue in vegetables evaluated by localized surface plasmon resonance of gold nanoparticles

Pakawat Kongpreecha, Sineenat Siri*

School of Biology, Institute of Science, Suranaree University of Technology, Nakhon Ratchasima 30000, Thailand

** Address for correspondence: Sineenat Siri, PhD, School of Biology, Institute of Science, Suranaree University of Technology, Nakhon Ratchasima 30000, Thailand. Tel: +66 89 7119112; e-mail: ssinee@sut.ac.th.*

Abstract

The contamination of paraquat in vegetables is widely concerned with human health risks, leading to the research interest in developing a paraquat sensing system. This work reported a simple detection of paraquat based on the electrostatic interaction of paraquat and the negatively charged gold nanoparticles (AuNPs), resulting in the changes of colors from red to blue and the shifting of localized surface plasmon resonance (LSPR) peaks of AuNPs. The limit of detection concentration (C_{LOD}) of this system was 100 µM paraquat. Moreover, among eight cationic salts tested, NaCl was selective to enhance the detection sensitivity of the system, resulting in the reduction of C_{LOD} to 0.10 µM. This system selectively detected paraquat, but not to other tested herbicides (ametryn, atrazine,

This article has been accepted for publication and undergone full peer review but has not been through the copyediting, typesetting, pagination and proofreading process, which may lead to differences between this version and the Version of Record. Please cite this article as doi: 10.1002/bab.2191.

glyphosate, and 2,4-D dimethyl ammonium). The paraquat-spiking experiment in kale demonstrated the significant recovery rate of paraquat at 96.0–103.0 %, and the relative standard deviations were less than 4%. The developed system was efficient for screening contaminated paraquat in vegetables under unwashed and washed conditions. Three out of five unwashed vegetables had a significant level of paraquat as determined by LSPR values. These results suggested the potential application of this system for a simple screening of contaminated paraquat in vegetables.

Keywords*: biosensor, detection, food safety, nanoparticles, paraquat, vegetables*

Abbreviations: *AuNPs****,*** *gold nanoparticles****;*** C_{LOD}***,*** *limit of detection concentration; LSPR, localized surface plasmon resonance.*

Highlights

- Simple paraquat-screening system was developed based on the negatively-charged gold nanoparticles.
- The limit of paraquat detection of this system was 0.10 μM.
- This system was potentially used for a simple screening of contaminated paraquat in vegetables.

1. Introduction

With a high expansion of population growth in each year, the increase of agricultural yield is globally on demand. Many synthetic chemicals for pest and weed controls are also increasingly applied to enhance agricultural productivity. The release of these chemicals to the environment [1] and their remaining residues in food can, directly and indirectly, affect human health. Therefore, food contamination and safety issues are extensive health care concerns worldwide [2]. Among these chemicals, paraquat (1,1′-dimethyl-4,4′-bipyridinium dichloride) is one of the most intercontinental used herbicides because of its effectiveness to kill green weed plants in agriculture [3]. Paraquat absorbed simply into the plant cells, and its high toxicity results from the disruption of intracellular electron transfer systems and induction of oxidative stress via increasing levels of reactive oxygen species (ROS) [4]. With its high solubility in water (700 g/L at 20 °C), slow degradation, and low volatility, paraquat directly harms the natural living organisms in the environment and indirectly affects human health from its residue in a food web [5]. Residues of paraquat can cause acute toxicity and long-term health effects depending on their levels in the human body. At a high level, acute toxicity may cause instant diarrhea and death. At a low level, paraquat can cause the long-term effects of lung injury [6], pulmonary fibrosis [7], and liver damage [8]. Also, the exposure of paraquat can associate with the increased risk of Parkinson's disease [9].

In many countries, paraquat contamination in vegetables is one of the great concerns in food safety. There were reports of the detection of contaminated paraquat in several vegetables collected from local markets and supermarkets, such as cabbage [10], tomato [11], round gourd [12], and adzuki beans [13]. Over a past decade, the paraquat detection techniques have been reported, including spectrophotometry [14], capillary

electrophoresis [15], gas chromatography [16], liquid chromatography [17], thin-layer chromatography [18], surface-enhanced Raman spectroscopy [19], and electrochemistry [20]. Although these techniques are effective for paraquat detection, their limitations are the requirement of an advanced instrument, high-cost expense, time-consuming process, in-laboratory detection, and requirement of a trained technician. Therefore, a simple, rapid, and on-site detection of paraquat has been a research challenge.

Colorimetric detection is one of the techniques suitable for a manageable and user-friendly detection system. With the unique optical property, gold nanoparticles (AuNPs) are commonly used for developing the colorimetric sensing of the targeted molecules [21]. The color transformation of AuNPs occurs according to their free (red color) and aggregated (blue color) forms. Several paraquat detection systems were developed via the use of AuNPs. The surface-enhanced Raman spectroscopy (SERS) technique was reported as an effective detection approach for paraquat, but this method required an advanced instrument for detecting [22]. Modified AuNPs with the synthetic receptor, aptamer, and sodium 3-mercaptopropanesulfonate were reported for the effective detection of paraquat [3, 23, 24]. Although these methods have high sensitivity for paraquat, they were still costly due to the addition of these complex molecules. Therefore, the low-cost system for paraquat screening has been a challenge, especially the contaminated paraquat in vegetables at the recommended value at 2 µM in at least 189 countries according to the Codex Alimentarius Commission [13]. Thus, this work aimed to develop a simple, cost-effective screening system for paraquat residue in vegetables, which was based on the coulombic attraction between negatively-charged AuNPs and paraquat under a salt-enhanced condition.

2. Materials and methods

2.1 Reagents

Gold (III) chloride trihydrate and paraquat were purchased from Sigma-Aldrich (St. Louis, MO, USA). Ammonium acetate, calcium chloride, lithium acetate, magnesium chloride, potassium chloride, sodium acetate, sodium chloride, sodium bicarbonate, sodium carbonate, and trisodium citrate dehydrate were bought from BDH (Poole, England). Glyphosate and 2,4-D dimethyl ammonium were obtained from Thaion Chemical (Bangkok, Thailand). Atrazine and ametryn were purchased from Chiatai (Bangkok, Thailand). Difenzoquat methyl sulfate was received from ChemCruz (Dallas, TX, USA).

2.2 Synthesis of citrate-capped AuNPs

One mL of 20 mM $HAuCl_4$ was added into the boiling deionized water (19 mL) with vigorous stirring before adding 2 mL of 58 mM sodium citrate. The formation of AuNPs was observed by the color change from yellow to colorless, dark blue, purple, and red, respectively. After boiling for 3 min, the reaction flask was removed from heat and allowed to cool down at room temperature. Subsequently, the pH of the solution was adjusted to 10.5 using 1 M sodium hydroxide with vigorous stirring, resulting in the change to deep red color.

2.3 Characterization

The formation of AuNPs was monitored by a UV-vis spectrum in a range of 300–900 nm using a UV-visible spectrometer (Analytik Jena Specord® 250 Plus, Jena, Germany) with a

resolution of 1 nm. The morphology and size of the synthesized AuNPs were analyzed by transmission electron microscope (TEM; Tecnai G2 S-Twin, FEI, Hillsboro, OR, USA) using a conventional transmission mode and an accelerating voltage of 200 kV. The sample was dropped on the carbon-coated copper grid and dried at ambient temperature before subjecting to TEM analysis. The ImageJ program (National Institutes of Health, Bethesda, MD, USA) was used to determine the average size of AuNPs from 100 particles at random locations of TEM images. The selected area electron diffraction (SAED) pattern was analyzed using a Tecnai G2 S-Twin TEM operating at 200 kV using LaB_6 filament. The crystallographic characterization of AuNPs was analyzed by X-ray diffraction (XRD) using a D8 Advance/Discover diffractometer (Bruker, Frankfurt, Germany) using a single crystal and wide-angle powder XRD method with Cu Kα radiation. The detection range of 2ϑ-diffraction angles was between 30° and 80° with a step-width $\Delta 2\vartheta$ of 0.02° and the sampling time was 10 s/step.

2.4 Sensitivity of detection

The sensitivity of the developed assay for paraquat detection was determined by mixing 100 µL paraquat at various concentrations (0, 20, 40, 80, 160, 240, and 320 µM) with 100 µL of AuNPs (9 nM) in a 96-well plate before incubating for 5 min at ambient temperature. The absorbance values at 690 and 520 nm (A_{690}/A_{520}) were used to determine the aggregated and free forms of AuNPs, respectively, which were measured by Bio Tek® microplate reader (Winooski, VT, USA). The UV-vis spectrum of each condition was also measured in a range of

300–900 nm using a UV-visible spectrometer. Also, to enhance the sensitivity of the developed assay, NaCl (20 mM) was added to the suspension of AuNPs. Then, 100 µL AuNPs (9 nM) were mixed with 100 µL paraquat at various concentrations (0, 0.5, 1.0, 2.0, 4.0, and 8.0 µM). After incubating for 5 min, the absorbance values of A_{690} and A_{520} were measured. The C_{LOD} and the minimum detectable signal of replicate blank readings (Y_{LOD}) were calculated using the equations (1) and (2), respectively. The equation (1) is to determine the concentration of paraquat at the C_{LOD}. The "a" represents the y-intercept and "b" represents the slope of the paraquat calibration curve that is plotted between A_{690}/A_{520} values and paraquat concentrations with the linear regression fit ($y = a + bx$) [25]. The equation (2) is to determine the minimum detectable signal of replicate blank readings (Y_{LOD}), where Y_{blank} is the average A_{690}/A_{520} value, and SD_{blank} is the standard deviation determined by a measurement of a blank sample in the condition without paraquat.

$$C_{LOD} = (Y_{LOD} - a)/b \quad \text{.....(1)}$$

$$Y_{LOD} = Y_{Blank} + 3SD_{Blank} \quad \text{.....(2)}$$

2.5 Selectivity of detection

The selectivity of the developed assay was determined by using five commonly used herbicides, including ametryn, atrazine, 2,4-D dimethyl ammonium, glyphosate, and paraquat. AuNPs (100 µL, 9 nM) with NaCl were mixed with each herbicide (100 µL, 40 µM) in a 96-well plate at ambient temperature for 5 min. The selectivity of the assay was determined by the ratio of A_{690}/A_{520} of each herbicide.

2.6 Recovery rate of spiked paraquat in organic kale

The paraquat-spiked experiment was performed to determine any interference of detection from the vegetable sample, which was interpreted by the recovery rate of the spiked paraquat. Paraquat (500 μL at 20, 40, and 80 μM) was put onto the leaves of organic kale (3 cm × 3 cm) and left at ambient temperature for 6 h. The method of paraquat extraction from the vegetable was adapted from Zou and colleagues [26]. Briefly, one gram of the organic kale was grounded before adding water (10 mL). The sample was incubated at 50 °C for 1 h in a sonication water bath. The extract solution was centrifuged at 6,000×*g* for 20 min before the collected supernatant was used for paraquat detection by the developed assay. AuNPs (100 μL, 9 nM) with NaCl were incubated with the extract solution (100 μL) in a 96-well plate at ambient temperature for 5 min. The absorbance values of A_{690} and A_{520} were measured. The recovery rate was calculated by the division between the measured concentration ($C_{measured}$) and the expected concentration ($C_{expected}$); the equation (3).

$$\text{Recovery rate} = (C_{measured} / C_{expected}) \times 100\% \quad \text{.....(3)}$$

2.7 Evaluation of paraquat residue in vegetables

The detection of paraquat residue in five common vegetables, collected from the local markets (cabbage, lettuce, sweet basil, kale, and cowpea), was carried out using the developed assay under the washed and unwashed conditions. Under a washed condition, vegetables were immersed in sodium bicarbonate for 15 min before rinsing three times with deionized water to remove any trace residues of sodium bicarbonate. The extract solution of each vegetable (1 g per 10 mL water) was incubated with AuNPs (100 μL, 9 nM) with NaCl in a 96-well plate at ambient temperature for 5 min before measuring A_{690} and A_{520}. The

A_{690}/A_{520} values were used to determine the paraquat concentration as compared with the standard curve.

2.8 Statistical Analysis

All experiments performed at least three replicates for determining the average and standard deviation. The statistical analysis was performed using SPSS 11.5 (SPSS, Chicago, IL, USA). The one-way ANOVA was used to analyze the variance of more than 2 sample groups, and Tukey's method was to compare the differences between all pairs of observations. The independent pair t-test was used to compare between 2 sample groups. The statistical difference is significant at $P < 0.05$.

3. Results and discussion

3.1 Synthesis and characterization of AuNPs

The AuNPs were synthesized and capped by citrate to provide the negatively-charged surface. The detection mechanism of paraquat by the developed system is shown in Fig. 1. The formation of AuNPs in the reaction was monitored via the observation of the color change, from transparent to red color, and the UV-Vis spectrum of the characteristic localized surface plasmon resonance (LSPR) peak [27]. As seen in Fig. 2A, the formation of AuNPs was indicated by the LSPR peak at 520 nm and the reaction appeared in red color. With the addition of paraquat, the LSPR peak was shifted to 690 nm and the solution color changed to blue. The average size of dispersive AuNPs was 12.80 ± 3.06 nm as determined by the measurement of 100 particles. Fig 2B revealed TEM images of AuNPs, in which dispersive and aggregated AuNPs were observed in the conditions without and with

paraquat, respectively.

Fig. 1

Fig. 2

The SAED and XRD analyses were used to confirm the identity of the synthesized AuNPs. Fig. 3A shows the SAED pattern of the synthesized AuNPs, which the diffraction spots distributed on concentric circles had the d values of 0.468, 0.418, 0.292, and 0.251 Å, corresponding to the (111), (200), (220), and (311) planes of Au^0, respectively [28]. The XRD pattern of the synthesized AuNPs illustrates in Fig. 3B, showing the diffraction peaks at 2-theta of 38.19°, 44.36°, 64.58°, and 77.79°, which were consistent with the (111), (200), (220), and (311) planes of the face-centered cubic (fcc) lattice of gold as compared with the standard database (Joint committee on powder diffraction standards (JCPDS) file No. 04–0784) [29].

Fig. 3

3.2 The developed system for paraquat detection

In this work, the paraquat detection system was based on the electrostatic interaction between the citrate-capped AuNPs and the positively-charged paraquat. As paraquat-induced aggregation of AuNPs, the color of AuNPs changed from red to blue according to their free and aggregated states, respectively. The detection feasibility of the developed system was investigated, as seen in Fig. 4A. The colorimetric detection depended on the paraquat concentration, in which the absorbance at 520 nm (free AuNPs) was gradually decreased, while the absorbance at 690 nm (aggregated AuNPs) was increased. The dynamic range of paraquat detection was determined, as shown in Fig. 4B. The linear

relationship between the A_{690}/A_{520} ratio and paraquat concentration was in a range of 80–320 µM, in which the calculated R^2 was 0.9959. The limit of detection concentration, C_{LOD}, of paraquat was 100 µM (or 25 ppm). The C_{LOD} of this system was lower than the C_{LOD} (389 µM or 100 ppm) of the previous report that was based on silver nanoparticles deposited on silicon (AgNPs@Si) couple with the surface-enhanced Raman scattering detecting technique [30].

Fig. 4

In this work, the cationic salts that could mediate the flocculation of AuNPs were included to enhance the sensitivity of detection of the developed system. Eight cationic salts at 5-30 mM were tested for their highest concentration to maintain a colloidal state of AuNPs; calcium chloride ($CaCl_2$), lithium acetate ($C_2H_3LiO_2$), magnesium chloride ($MgCl_2$), potassium chloride (KCl), sodium acetate ($C_2H_3NaO_2$), ammonium acetate ($C_2H_7NO_2$), sodium chloride (NaCl), and sodium carbonate (Na_2CO_3). As seen in Fig. 5A, lithium acetate and sodium acetate could maintain the colloidal state of AuNPs at the highest concentration of 30 mM, followed by sodium chloride (20 mM). However, with the addition of paraquat (Fig. 5B), both lithium acetate and sodium acetate could not induce the aggregation of AuNPs. Instead, sodium chloride could cause AuNP-aggregation, so it was chosen for enhancing the sensitivity of detection of the developed system. Lithium ions may be less effective for inducing the aggregation of AuNPs because of their smaller size and feasible formation of a non-covalent bond with water [31]. Also, acetate ions can be adsorbed on the surface of AuNPs, making great prevention of the aggregation of AuNPs [32]. Therefore, both lithium acetate and sodium acetate were not suitable to use as a flocculation inducer in this work. For sodium chloride, both sodium and chloride ions are small and easy to form a non-

covalent bond with water, thus being less effective to induce the aggregation of AuNPs as compared with lithium acetate and sodium acetate. For other salts, they were not chosen since they could induce the aggregation of AuNPs in the condition without paraquat. For sodium carbonate, two sodium ions likely provide greater force to induce aggregation of AuNPs. For potassium chloride, potassium ions have a larger size than sodium ions, making them better induce aggregation of AuNPs. For calcium chloride and magnesium chloride, both divalent cations can induce the aggregation of AuNPs better than monovalent sodium ions [33].

Fig. 5

The detection-enhanced system with the additional NaCl was investigated for paraquat detection. Fig. 6A shows the UV-vis spectra of the NaCl-treated AuNPs incubating with various concentrations (20–320 µM) of paraquat. With 20 mM NaCl, AuNPs appeared in red, which the SPR peak remained at 520 nm. AuNPs were induced to aggregate when paraquat was added as low as 20 µM, which the reaction color was turned from red to blue. This paraquat detection was four times lower than the previous detection without NaCl. The linear relationship between the A_{690}/A_{520} and paraquat concentration was in a range of 0.5–8.0 µM with the calculated R^2 of 0.9908 (Fig. 6B). The calculated C_{LOD} was reduced to 0.10 µM (or 0.025 ppm), indicating the increased sensitivity of the detection by this developed system. This improved sensitivity was likely resulted from the negative charges on the surface of AuNPs disturbed by Na^+ from NaCl [34]. Thus, the stabilization of citrate on the surface of AuNPs decreases, resulting in faster induced-aggregation of AuNPs upon the presence of paraquat. As compared with the conventional sodium dithionite assay, this

developed system has the lower sensitivity of detection, in which the sodium dithionite assay has the detection sensitivity at 1.24 mg L^{-1} (4.81 µM or 1.24 ppm) [35]. It was noted the maximum residue limit (MRL) of paraquat in agricultural products by official regulations varied in each country. Nevertheless, the MRL of paraquat is set at 2 µM in at least 189 countries, according to the Codex Alimentarius Commission [13, 36]. Thus, the developed system was potentially used as a simple system for paraquat screening as its C_{LOD} was as low as 0.10 µM.

Fig. 6

3.4 Selectivity of detection

The selectivity of detection of the developed assay was determined by testing with five herbicides commonly used in Asian agriculture. The tested herbicides include the positively charged herbicides (paraquat, atrazine, and ametryn) and negatively charged herbicides (glyphosate and 2,4-D dimethyl ammonium). Fig. 7 shows the detection selectivity of the developed system, which is determined by the A_{690}/A_{520} ratio. The developed approach was exclusively detected paraquat, but not the other positively charged herbicides (atrazine and ametryn), nor the negatively charged herbicides (glyphosate and 2,4-D dimethyl ammonium). Although atrazine and ametryn were positive charges, their structures were a steric hindrance and difficult to interact with AuNPs. Therefore, both chemicals did not induce the aggregation of AuNPs. In contrast, paraquat has the rotated pyrimidine rings with the two positions of nitrogen cations that can interact with the negative charges of citrate-capped AuNPs through the electrostatic interaction [37]. In addition, paraquat has a planar geometry and a less steric hindrance, thus easily access the surface of AuNPs and induce their aggregation. Glyphosate and 2,4-D dimethyl ammonium exhibited the negative

charges due to the hydroxyl group of glyphosate and oxygen and chloride atoms of 2,4-D dimethyl ammonium. The negative charges of these herbicides are impulsive to the citrate-capped AuNPs.

Fig. 7

3.5 Evaluation of the developed system to detect paraquat in vegetables

Different amounts of paraquat (1.0, 2.0, and 4.0 μM) were spiked on the organic kale (without herbicide usage) to evaluate the analytical performance of the developed detection system. The results are shown in Table 1, in which the detection results were also compared with the HPLC analysis. The recovery rate of this assay to detect the spiked paraquat in the kale samples was in a range of 96.0–103.0%, and relative standard deviation (RSD) values were lower than 4%, suggesting a minute interfering effect of the vegetable color and components on the detection. The development method was compared with other paraquat detection methods as shown in Table 2. Although the LOD of the developed method is not the lowest as compared with the previous report, its detection sensitivity is higher than many other detection methods. Its LOD at 0.1 μM is applicable for the detection of contaminated paraquat in vegetables, which the MRL of paraquat in agricultural products mostly regulates at 2 μM, according to the Codex Alimentarius Commission [13, 36]. Also, the developed system has advantages in its low cost and rapid colorimetric detection of paraquat in vegetable samples.

Table 1

Table 2

The developed system was further tested for the contaminated paraquat in five vegetables collected from local markets; cabbage, lettuce, sweet basil, kale, and cowpea.

The vegetable samples were prepared as unwashed and washed ones. Under a wash condition, the samples were washed once with sodium bicarbonate for 15 min and rinsed with DI water according to the recommendation by the Thai Health Promotion Foundation. The results show in Fig. 8, in which the contaminated paraquat as clearly seen by naked eyes (blue color) was found only in the unwashed cowpea sample. However, as determined by the A_{690}/A_{520} ratio, paraquat was also detected in the unwashed kale and sweet basil samples. The highest detection of contaminated paraquat was found in the unwashed cowpea (6.96 ± 0.14 µM), followed by the unwashed kale (1.24 ± 0.15 µM) and the unwashed sweet basil (0.60 ± 0.06 µM), respectively. In washed vegetables, no detection of paraquat was detected as it was washed out from the surfaces of vegetables by sodium bicarbonate and water.

Fig. 8

4. Conclusion

This work demonstrated a simple, sensitive system for paraquat screening based on the use of citrate-capped AuNPs with the presence of NaCl. With paraquat, AuNPs were induced to aggregate, resulting in the changes of color from red to blue. The developed system had the detection sensitivity for paraquat at 0.10 µM. It was selective to paraquat, but not other commonly used herbicides in Asia agriculture, including atrazine, ametryn, 2,4-D dimethyl ammonium, and glyphosate. In the paraquat-spiked kale samples, this system showed an efficient recovery rate of paraquat in a range of 89–107% and the low relative standard deviation (RSD) values of less than 4%. This developed system was used to screen the paraquat-contaminated vegetables collected from local markets; cabbage, lettuce, sweet

basil, kale, and cowpea. This system suggested three-positive vegetables with contaminated paraquat under the unwashed condition. These results suggested the potential application of the developed system as a simple system to screen for contaminated paraquat in vegetables.

5. Acknowledgments

This work is supported by the Fundamental Fund, the Suranaree University of Technology.

The authors declare no conflict of interest.

6. References

[1] Falahati-Pour, S. K., Lotfi, A. S., Ahmadian, G., Baghizadeh, A., Behroozi, R., Haghighi, F. (2016) Biotechnol. Appl. Biochem. 63, 870-876.

[2] Szarka, A., Búčiková, K., Kostić, I., Hrouzková, S. (2020) Food. Anal. Method. 13, 1829-1841.

[3] Shan, X., de Dieu Habimana, J., Ji, J., Sun, J., Pi, F., Zhang, Y., Sun, X. (2019) J. Solid. State. Electrochem. 23, 1211-1220.

[4] Zhan, Y., Guo, Z., Zheng, F., Zhang, Z., Li, K., Wang, Q., Wang, L., Cai, Z., Chen, N., Wu, S., Li, H. (2020) Environ. Toxicol., 1-10.

[5] Sartori, F., Vidrio, E. (2018) Toxicol. Environ. Chem. 100, 479-517.

[6] Yan, B., Chen, F., Xu, L., Xing, J., Wang, X. (2017) Sci. Rep. 7, 597.

[7] Tai, W., Deng, S., Wu, W., Li, Z., Lei, W., Wang, Y., Vongphouttha, C., Zhang, T., Dong, Z. (2020) J. Cell. Physiol. 235, 1759-1768.

[8] Eftekhari, A., Hasanzadeh, A., Khalilov, R., Hosainzadegan, H., Ahmadian, E., Eghbal, M. A. (2020) Environ. Sci. Pollut. Res. Int. 27, 4969-4975.

[9] Reczek, C. R., Birsoy, K., Kong, H., Martínez-Reyes, I., Wang, T., Gao, P., Sabatini, D. M., Chandel, N. S. (2017) Nat. Chem. Biol. 13, 1274-1279.

[10] Osman, K., Al-Humaid, A., Al-Rehiayani, S., Al-Redhaiman, K. (2010) Ecotoxicol. Environ. Saf. 73, 1433-1439.

[11] Farahi, A., Achak, M., El Gaini, L., El Mhammedi, M. A., Bakasse, M. (2016) Food. Anal. Method. 9, 139-147.

[12] Akhtar, S., Yaqub, G., Hamid, A., Afzal, Z., Asghar, S. (2018) Curr. World. Environ. 13, 242-250.

[13] Tsen, C. M., Yu, C.-W., Chuang, W.-C., Chen, M.-J., Lin, S.-K., Shyu, T.-H., Wang, Y.-H., Li, C.-C., Chao, W.-C., Chuang, C.-Y. (2019) Analyst. 144, 426-438.

[14] Siangproh, W., Somboonsuk, T., Chailapakul, O., Songsrirote, K. (2017) Talanta. 174, 448-453.

[15] Vu, A. P., Nguyen, T. N., Do, T. T., Doan, T. H., Ha, T. H., Ta, T. T., Nguyen, H. L., Hauser, P. C., Nguyen, T. A. H., Mai, T. D. (2017) J. Chromatogr. B. 1060, 111-117.

[16] Lamei, N., Ezoddin, M., Kakavandi, N. R., Abdi, K., Ghazi-khansari, M. (2018) Chromatographia. 81, 923-930.

[17] Bauer, A., Luetjohann, J., Rohn, S., Kuballa, J., Jantzen, E. (2018) Food. Anal. Method. 11, 2237-2243.

[18] Pathan, A. M., Baseer, M. A., Kadam, A. B., Junne, S. B. (2019) JPC-J. Planar. Chromat. 32, 335-338.

[19] Botta, R., Eiamchai, P., Horprathum, M., Limwichean, S., Chananonnawathorn, C., Patthanasettakul, V., Maezono, R., Jomphoak, A., Nuntawong, N. (2020) Sens. Actuators. B. Chem. 304, 127327.

[20] Pourakbari, Z., Sheykhan, M., Aliakbar, A. (2020) J. Environ. Chem. Eng. 8, 104284.

[21] Ahmad, T., Bustam, M. A., Irfan, M., Moniruzzaman, M., Asghar, H. M. A., Bhattacharjee, S. (2019) Biotechnol. Appl. Biochem. 66, 698-708.

[22] Luo, H., Wang, X., Huang, Y., Lai, K., Rasco, B. A., Fan, Y. (2018) J. Sci. Food. Agric. 98, 3892-3898.

[23] Ran, X.-D., Wu, Y.-G. (2019) Chin. J. Anal. Chem. 47, 567-575.

[24] Zhang, Y., Huang, Y., Fu, L., Qiu, J., Wang, Z., Wu, A. (2020) J. Food. Compost. Anal. 92, 103574.

[25] Gumustas, M., Ozkan, S. A. (2011) Open. Anal. Chem. J. 5, 1-21.

[26] Zou, T., He, P., Cao, J., Li, Z. (2014) J. Chromatogr. Sci. 53, 204-209.

[27] Lee, J. H., Choi, S. U., Jang, S. P., Lee, S. Y. (2012) Nanoscale. Res. Lett. 7, 420.

[28] Mevold, A. H., Hsu, W.-W., Hardiansyah, A., Huang, L.-Y., Yang, M.-C., Liu, T.-Y., Chan, T.-Y., Wang, K.-S., Su, Y.-A., Jeng, R.-J. (2015) Nanoscale. Res. Lett. 10, 1-7.

[29] Krishnamurthy, S., Esterle, A., Sharma, N. C., Sahi, S. V. (2014) Nanoscale. Res. Lett. 9, 627.

[30] Dao, T. C., Luong, T. Q. N., Cao, T. A., Nguyen, N. H., Kieu, N. M., Luong, T. T., Le, V. V. (2015) Adv. Nat. Sci: Nanosci. Nanotechnol. 6, 035012.

[31] Liu, B., Kelly, E. Y., Liu, J. (2014) Langmuir. 30, 13228-13234.

[32] Al-Johani, H., Abou-Hamad, E., Jedidi, A., Widdifield, C. M., Viger-Gravel, J., Sangaru, S. S., Gajan, D., Anjum, D. H., Ould-Chikh, S., Hedhili, M. N. (2017) Nat. Chem. 9, 890-895.

[33] Hu, S., Huang, P. J. J., Wang, J., Liu, J. (2020) Anal. Chem. 19, 13354–13360.

[34] Dominguez-Medina, S., Blankenburg, J., Olson, J., Landes, C. F., Link, S. (2013) ACS Sustain. Chem. Eng. 1, 833-842.

[35] Chaikhan, P., Udnan, Y., Sananmuang, R., Ampiah-Bonney, R. J., Chuachuad Chaiyasith, W. (2020) Microchem. J. 159, 105355.

[36] Lima, T., Nicoletti, M., Munhoz, C., Abreu, G., Magalhães, J., Ricci, E., Waziry, P., Costa, J., Antônio, A., Fukushima, A. (2018) Food. Nutr. Sci. 9, 1368-1375.

[37] Kumar, N., Seth, R., Kumar, H. (2014) Anal. Biochem. 456, 43-49.

[38] Chaikhan, P., Udnan, Y., Sananmuang, R., Ampiah-Bonney, R. J., Chaiyasith, W. C. (2020) Microchem. J. 159, 105355.

[39] Vu, A. P., Nguyen, T. N., Do, T. T., Doan, T. H., Ha, T. H., Ta, T. T., Nguyen, H. L., Hauser, P. C., Nguyen, T. A. H., Mai, T. D. (2017) J. Chromatogr. B. 1060, 111-117.

[40] Pacheco, M. R., Barbosa, S. C., Quadrado, R. F. N., Fajardo, A. R., Dias, D. (2019) Anal. Bioanal. Chem. 411, 3269-3280.

[41] de Almeida, R. M., Yonamine, M. (2007) J. Chromatogr. B. 853, 260-264.

[42] Asgari, S., Sun, L., Lin, J., Weng, Z., Wu, G., Zhang, Y., Lin, M. (2020) Microchim. Acta. 187, 390.

[43] Zhang, W., Su, Y., Shi, J., Zhang, M., Wu, B., Chen, S., Hu, S., Rao, Z., Zheng, J. (2014) Anal. Methods. 6, 6560-6564.

[44] Gusrizal, G., Santosa, S. J., Kunarti, E. S., Rusdiarso, B. (2019) Indones. J. Chem. 20, 688-696.

[45] Ali, S., Shah, M. R., Hussain, S., Khan, S., Latif, A., Ahmad, M., Ali, M. (2021) J. Clust. Sci., 1-8.

[46] Rohit, J. V., Kailasa, S. K. (2014) J. Nanopart. Res. 16, 1-16.

[47] Kuitio, C., Klangprapan, S., Chingkitti, N., Boonthavivudhi, S., Choowongkomon, K. (2021) J. Environ. Sci. Health. B., 1-8.

[48] Zhang, Y., Huang, Y., Fu, L., Qiu, J., Wang, Z., Wu, A. (2020) J. Food. Compost. Anal. 92, 103574.

Table captions

Table 1 Paraquat determination in the paraquat-spiked vegetable using the developed system.

Sample	Paraquat added (μM)	HPLC (μM)	The developed method (μM)	Recovery (%)	RSD (%) [n]
Kale	1.0	0.92	1.03±0.02	103.0	1.94
	2.0	1.83	1.94±0.07	96.0	3.61
	4.0	3.82	3.86±0.15	96.5	3.87

Relative standard deviation (RSD), n=3.

Table 2 Comparison of paraquat detection methods.

Detection technique	System	LOD (μM)	References
Microfluidic paper-based analytical device	Sodium dithionite reaction	4.82	[38]
Capillary electrophoresis	CE–C^4D	1.94	[39]
Electrochemistry	ALG–GA–CB/GCE	0.23	[40]
Gas chromatography	GC–MS	0.19	[41]
Surface-enhanced Raman spectroscopy	NFC/Au@Ag NP nanocomposite	0.18	[42]
Liquid chromatography	HPLC	0.10	[43]
Colorimetry	*p*-Hydroxybenzoic Acid–AgNPs	8.30	[44]
Colorimetry	Imida–AgNPs	6.27	[45]
Colorimetry	CN-DTC–AgNPs	7.21	[46]
Colorimetry	Aptamer–AuNPs	1.04	[47]
Colorimetry	3MPS–AuNPs	0.0039	[48]
Colorimetry	Citrate–AuNPs	0.10	This work

Figure captions

Fig. **1** Mechanism of the developed system to detect paraquat.

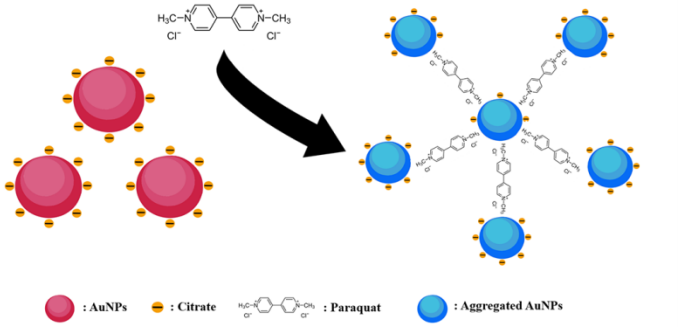

Fig. **2** UV-Vis spectra (A) and TEM images (B) of the synthesized AuNPs in the conditions without and with paraquat.

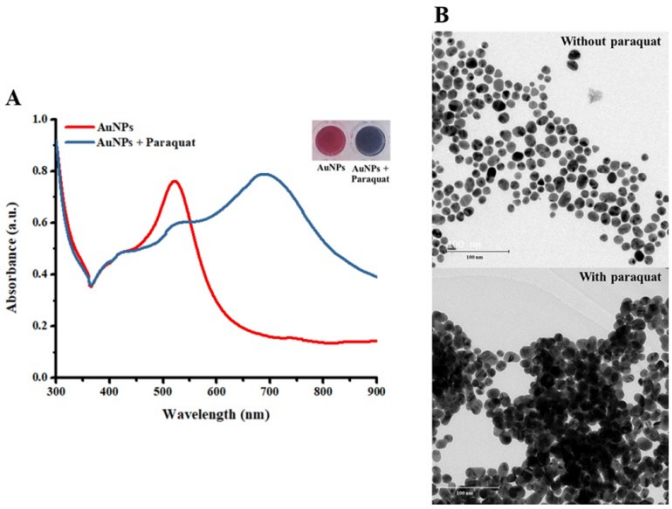

Fig. 3 The crystalline structure of the synthesized AuNPs analyzed by SAED-TEM (A) and XRD (B).

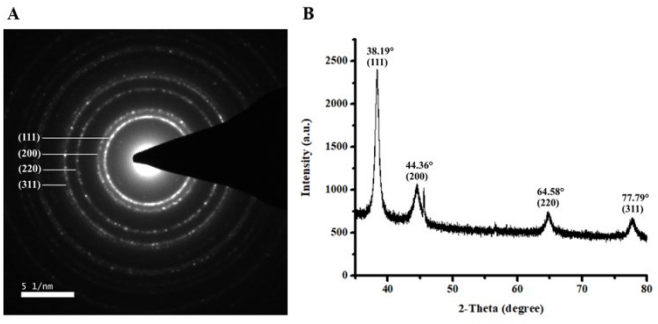

Fig. **4** UV-Vis spectra (A) and sensitivity of detection for paraquat (B) of the developed system.

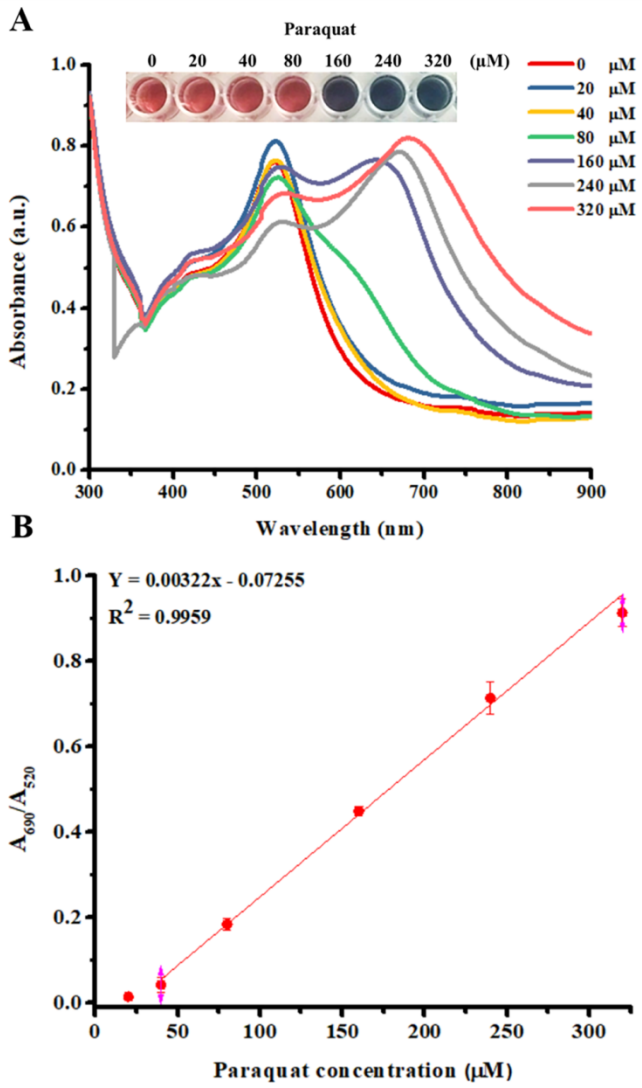

Fig. **5** Salt-induced aggregation of AuNPs under the conditions with (A) and without (B) paraquat.

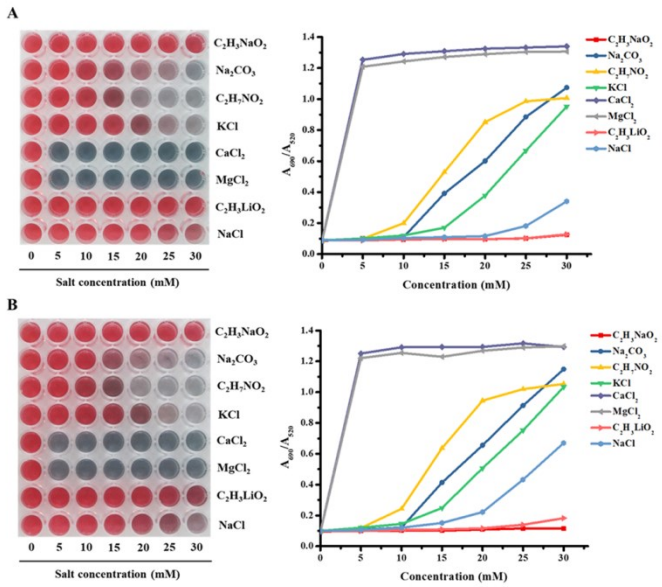

Fig. **6** UV-vis spectra (A) and sensitivity of detection for paraquat (B) of the developed system with addition of NaCl.

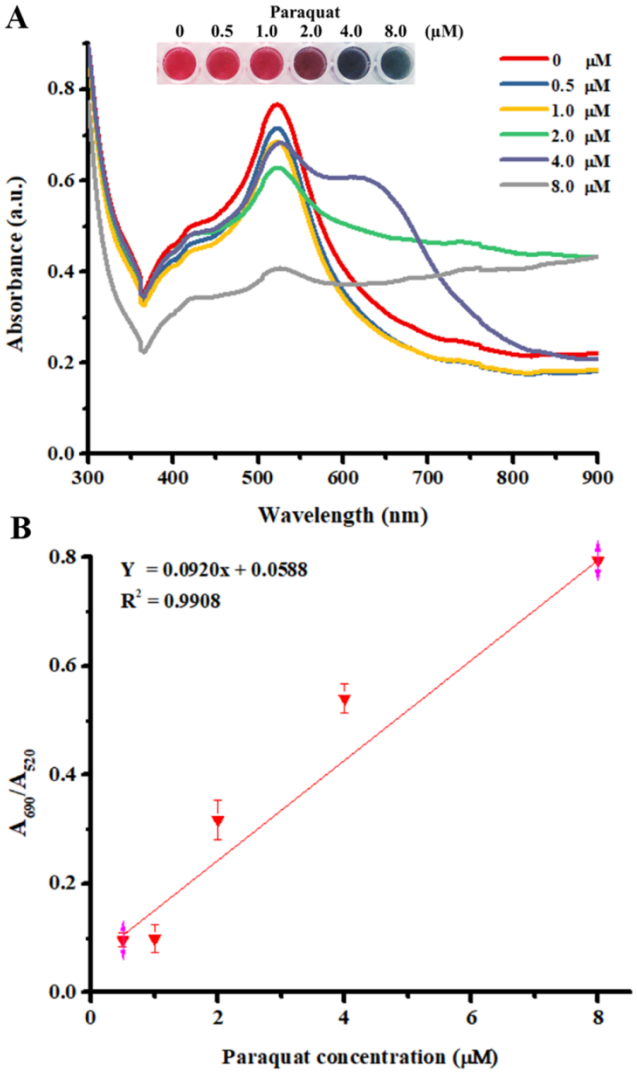

Fig. **7** Selectivity of the developed system to paraquat as compared with other common herbicides.

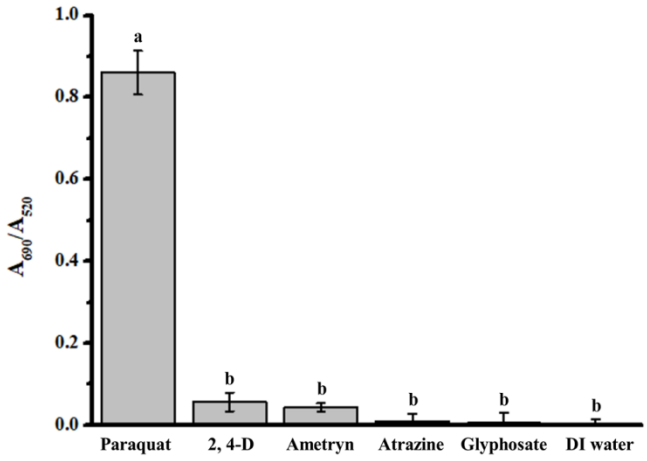

Fig. 8 Paraquat detection in five vegetables collected from local markets using the developed system.